

PAPER • OPEN ACCESS

# Core-hole localization and ultra-fast dissociation in $\text{SF}_6$






To cite this article: V Ekholm *et al* 2020 *J. Phys. B: At. Mol. Opt. Phys.* **53** 185101

View the [article online](#) for updates and enhancements.

## You may also like

- [Hard x-ray spectroscopy and dynamics of isolated atoms and molecules: a review](#)  
M N Piancastelli, T Marchenko, R Guillemin *et al.*
- [Electronic and crystal structures of  \$\text{LnFeAsO}\_{4-x}\text{H}\_x\$  \( \$\text{Ln} = \text{La, Sm}\$ \) studied by x-ray absorption spectroscopy, x-ray emission spectroscopy, and x-ray diffraction \(part I: carrier-doping dependence\)](#)  
Yoshiya Yamamoto, Hitoshi Yamaoka, Takayuki Uozumi *et al.*
- [Effect of broken symmetry on resonant inelastic x-ray scattering from undoped cuprates](#)  
Jun-ichi Igarashi and Tatsuya Nagao

# Core-hole localization and ultra-fast dissociation in SF<sub>6</sub>

V Ekholm<sup>1,2</sup> , G S Chiuzbăian<sup>3,4</sup>, C Săthe<sup>1</sup> , A Nicolaou<sup>4</sup>, M Guarise<sup>3,5</sup>,  
M Simon<sup>3</sup> , N Jaouen<sup>4</sup> , J Lüning<sup>3</sup>, C F Hague<sup>3</sup>, F Gel'mukhanov<sup>6,7,8</sup>,  
M Odelius<sup>9</sup> , O Björneholm<sup>2</sup> and J-E Rubensson<sup>2</sup>

<sup>1</sup> MAX IV Laboratory, Lund University, Box 118, SE-221 00 Lund, Sweden

<sup>2</sup> Department of Physics and Astronomy, Uppsala University, Box 516, SE-751 20 Uppsala, Sweden

<sup>3</sup> Sorbonne Université and CNRS, Laboratoire de Chimie Physique-Matière et Rayonnement, LCPMR, F-75005, Paris, France

<sup>4</sup> Synchrotron SOLEIL, L'Orme des Merisiers, Saint-Aubin, B. P. 48, 91192 Gif-sur-Yvette, France

<sup>5</sup> Centro Nacional de Pesquisa em Energia e Materiais (CNPEM), 10000 Campinas, Brazil

<sup>6</sup> Theoretical Chemistry & Biology, School of Biotechnology, Royal Institute of Technology, S-106 91 Stockholm, Sweden

<sup>7</sup> Siberian Federal University, 660041 Krasnoyarsk, Russia

<sup>8</sup> Kirensky Institute of Physics, Federal Research Center KSC SB RAS, 660036 Krasnoyarsk, Russia

<sup>9</sup> Department of Physics, AlbaNova University Center, Stockholm University, SE-106 91 Stockholm, Sweden

E-mail: [victor.ekholm@maxiv.lu.se](mailto:victor.ekholm@maxiv.lu.se), [odelius@fysik.su.se](mailto:odelius@fysik.su.se) and [jan-erik.rubensson@physics.uu.se](mailto:jan-erik.rubensson@physics.uu.se)

Received 25 March 2020, revised 16 June 2020

Accepted for publication 2 July 2020

Published 24 July 2020



## Abstract

Resonant inelastic x-ray scattering spectra excited at the fluorine K resonances of SF<sub>6</sub> have been recorded. While a small but significant propensity for electronically parity-allowed transitions is found, the observation of parity-forbidden electronic transitions is attributed to vibronic coupling that breaks the global inversion symmetry of the electronic wavefunction and localizes the core hole. The dependence of the scattering cross section on the polarization of the incident radiation and the scattering angle is interpreted in terms of local  $\pi/\sigma$  symmetry around the S–F bond. This symmetry selectivity prevails during the dissociation that occurs during the scattering process.


**Keywords:** SF<sub>6</sub>, resonant inelastic x-ray scattering, symmetry selection rules, ultrafast dynamics, vibronic couplings

(Some figures may appear in colour only in the online journal)

## 1. Introduction

Electronic states in an inversion-symmetric system have well-defined parity. Hence, a fluorine 1s core hole in the SF<sub>6</sub> molecule is typically described in terms of a multiconfigurational symmetry-adapted wavefunction, comprising core holes at various fluorine sites. If inversion symmetry is broken the sites become inequivalent and the core hole can localize

[1, 2]. In resonant inelastic x-ray scattering (RIXS) symmetry breaking due to ultrafast electronic–vibronic coupling is manifested in population of electronically parity forbidden final states [3–5]. Even in such cases, however, RIXS spectra are sensitive to the symmetry of the wavefunction. There is still a propensity for populating ‘allowed’ relative to ‘forbidden’ [3] final states if the geometry is close to being inversion symmetric. Moreover, the *local* symmetry of molecular orbitals can be probed by varying the angle between the polarization direction of the incident radiation and the direction of the scattered radiation. Symmetry considerations are essential in many fields of physics, and the role of global and local symmetry has

 Original content from this work may be used under the terms of the [Creative Commons Attribution 4.0 licence](https://creativecommons.org/licenses/by/4.0/). Any further distribution of this work must maintain attribution to the author(s) and the title of the work, journal citation and DOI.

e.g., been investigated for transmission and reflection in scattering systems [6, 7]. The global symmetry breaking discussed in this paper concerns the electronic part of the wavefunction, while the symmetry selectivity due to the dipole approximation (dipole selection rules) may very well be operational for the total wavefunction which includes both electronic and vibronic degrees of freedom [5, 8].

In a crude ionic picture each F atom in SF<sub>6</sub> has a filled 2p shell, with atomic orbitals oriented either parallel or perpendicular to the S–F bond forming local  $\sigma$  or  $\pi$  type bonds, respectively. Electrostatic interactions and covalency lift the degeneracy so that molecular orbitals of various symmetry are energetically separated. Together with the relative simplicity of  $s \leftrightarrow p$  transitions and the initial inversion symmetry, this makes the SF<sub>6</sub> molecule a showcase for symmetry sensitivity in RIXS. x-ray emission spectra (XES) of SF<sub>6</sub> have earlier been measured with electron excitation [9, 10], and RIXS have been measured at the K edge [11] and the L edge [12, 13] of sulfur.

Here we present RIXS spectra of SF<sub>6</sub> excited in the vicinity of the F K edge. Indeed, electronically dipole forbidden transitions are observed, demonstrating dynamic breaking of the global electronic inversion symmetry and suggesting core-hole localization. Only a small but significant propensity for parity allowed transitions is found. A dependence of the polarization of the incident radiation is observed, which is interpreted in terms local dipole selection rules related to the local  $\pi/\sigma$  symmetry around the S–F bond. Analysis of the electron emission has earlier demonstrated that dissociation can occur prior to the core hole decay [14–17], and indeed a sharp peak suggesting atomic transitions is observed in the present RIXS spectra. The polarization dependence indicates that local  $\pi/\sigma$  symmetry is retained, and our analysis shows that the sharp peak primarily is associated with emission at large interatomic distances during dissociation.

## 2. Experimental

RIXS spectra were measured at the F K edge using the AERHA spectrometer [20] mounted at the SEXTANTS beamline [21] of the SOLEIL light source and a gas cell with a 100 nm thick Si<sub>3</sub>N<sub>4</sub> membrane, through which both primary and secondary radiation penetrated. The SF<sub>6</sub> sample pressure was 1 bar, and the angle between the incident radiation and the membrane surface was 25°. At a scattering angle of 85°, spectra were measured with both vertical and horizontal linear polarization of the incident radiation.

The absolute energy scale of the monochromator was calibrated by matching the fluorescence yield spectrum to the published x-ray absorption spectrum in reference [22]. The spectrometer energy scale was tied to the monochromator energy via elastic scattering. From the elastic peaks the overall energy resolution was estimated to be 0.3 eV.

The XES spectrum is best aligned to the valence-band photoemission spectrum (PES) [18] using 694.6 eV for the F 1s binding energy, which complies with the value given by Siegbahn *et al* [19]. A precise determination of the BE from XES is hampered as the ionisation is accompanied by a large

number of unresolved vibrational excitations that contribute to the width and the general shape of the PES peak. Whether the adiabatic or the vertical binding energy is the most appropriate reference for XES is influenced by the excitation–emission dynamics, and our results do not rule out other determinations of the fluorine 1s binding energy [23, 24].

## 3. Theory

The local symmetry and character of different transitions are analyzed in the molecular orbital frame work of the electronic ground state, augmented with classical simulations of dynamical effects in the core-ionized state, as employed in previous studies of complex systems [25, 26]. The electronic structure of the SF<sub>6</sub> molecule was described on the level of density functional theory in the CP2K software suite (version 6.0) [27–30] using the Gaussian augmented plane wave (GAPW) method [31], the hybrid PBE0 functional [32, 33] and aug-cc-VTZP basis sets [34]. A hybrid functional was required to obtain a good description of the chemical bonding and an accurate ground state geometry. Combined with the Gaussian basis, an auxiliary plane wave basis (with a cut-off of 600 Ry) was used to describe the electron density in a cubic simulation cell of dimension 20 Å, combined with a Poisson solver to model isolated systems [35]. The geometry optimization yields O<sub>h</sub> symmetry and a S–F bond distance of 1.575 Å, which compares well with the experimental value of 1.564 Å [36].

Simulated fluorine K-edge XES were derived from ground state Kohn–Sham orbitals as implemented in the GAPW method [37]. The discrete XES transitions and the density of states were convoluted with a Gaussian broadening with a full-width half-maximum of 0.3 eV and ad hoc energy shifts were added for direct comparison to the measured XES and PES spectra. However, the shifts were chosen such that the theoretical PES and XES spectra are aligned in figure 1, since in the absence of dynamical effects they are modelled on the basis of the same Kohn–Sham orbitals. The influence of nuclear dynamics during the core-hole lifetime was investigated classically by performing classical *ab initio* molecular dynamics simulations to follow the dynamics in the F 1s core ionized state, in analogy with previous XES simulations [25]. The core ionization was modelled in the  $Z + 1$  approximation by replacing SF<sub>6</sub> with SF<sub>5</sub>Ne<sup>+</sup>. The core-excited state trajectory was followed for 20 fs with a time-step of 0.5 fs which is sufficient for capturing nuclear dynamics during an estimated F 1s lifetime with an exponential decay of 3.3 fs [17]. The XES spectra of SF<sub>6</sub> were calculated for configurations along the trajectory in the core-ionized state and used for deriving a life-time average according to the exponential decay.

## 4. Results and discussion

The XES spectrum excited at 751.4 eV, far above any sharp resonances, is dominated by a 3–4 eV broad structure peaking at around 678 eV (figure 1). This peak can be attributed to

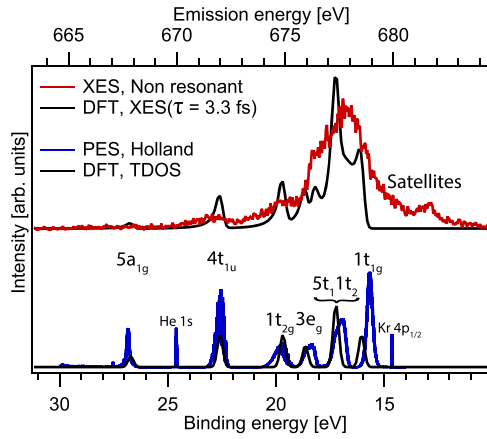


**Figure 1.** The F K-edge XES of  $\text{SF}_6$  excited at 751.4 eV is presented together with the experimental PES [18]. The XES spectrum is aligned to the PES spectrum using 694.6 eV for the core level binding energy [19]. The theoretical spectra are shifted to fit the experimental PES.

transitions from the F 1s core hole states to states with a hole in F 2p-derived outer orbitals.

In a pure ionic-bond picture the  $\text{SF}_6$  molecule binds the  $\text{S}^{6+}$  and  $\text{F}^-$  closed shell atoms. It has  $O_h$  symmetry with the formal electronic configuration:

$$1a_{1g}^2(1s^2)2a_{1g}^2 1e_g^4 1t_{1u}^6 (\text{F}1s^{12}) 3a_{1g}^2 (2s^2) 2t_{1u}^6 (2p^6) 4a_{1g}^2 3t_{1u}^6 2e_g^4 (\text{F}2s^{12}) 5a_{1g}^2 4t_{1u}^6 1t_{2g}^6 3e_g^4 5t_{1u}^6 1t_{2u}^6 1t_{1g}^6 (\text{F}2p^{36}).$$

Assuming that the symmetry is unbroken the fluorine core orbitals are of  $a_{1g}$ ,  $e_g$  and  $t_{1u}$  symmetry. States with core vacancy of corresponding symmetries can be built in linear combinations of local F 1s hole states, and vice versa. As emission associated with electron transfer from all valence orbitals to the core levels is allowed, and as there is no significant symmetry selectivity for excitation high above the ionization limit the discussion of local versus global symmetry selectivity becomes irrelevant for the high-energy excited spectrum. This will, however, become crucial in the discussion of the resonantly excited spectra, and for this purpose we show the Kohn–Sham valence orbitals in figure 2. S–F bonding/antibonding combinations involving sulfur 3s orbitals constitute orbitals of  $a_{1g}$  symmetry, which for local S–F bonds unambiguously give  $\sigma$  symmetry (figure 2). Bonding/antibonding combinations with S 3p are of  $t_{1u}$  symmetry, and as seen in figure 2 this global symmetry allows for both  $\pi$  and  $\sigma$  local S–F symmetry. A feature corresponding to the bonding  $4t_{1u}$  orbital is found around 672 eV emission (figure 1). There are weaker S–F interactions allowed via S 3d combinations giving rise to  $3e_g$  with local  $\sigma$  symmetry and  $1t_{2g}$  with local  $\pi$  character, with intensity found at 675 eV emission energy (figure 1). The other global symmetries primarily correspond to ‘non-bonding’ orbitals. The  $1t_{1g}$  and  $1t_{2u}$  orbitals correspond to f symmetry at the sulfur, and are non-bonding, whereas  $5t_{1u}$  is simply strongly localized on fluorine. In the calculations, we observe that the  $4t_{1u}$  has strong  $\sigma$  character and that  $5t_{1u}$  has predominantly  $\pi$  character. Intensity corresponding to the ‘non-bonding’ orbitals make up the main 3–4 eV broad structure in the emission spectrum peaking at

around 678 eV (figure 1). Notice that the corresponding anti-bonding  $a_{1g}^*$ ,  $t_{1u}^*$  and  $t_{2g}^*$  and  $e_g^*$  orbitals are unoccupied, and available for excitation in x-ray absorption.

The assignment of the features in the XES spectrum (figure 1) is accomplished by comparing to the He II excited PES of reference [18], and our theoretical analysis based on DFT calculations. The simulated XES and total density of states (TDOS) are aligned to the PES spectrum while the alignment of the two experimental scales corresponds to a F 1s binding energy of 694.6 eV.

Apart from the main features a satellite assigned to multiple excitations in the excitations step is found at 681 eV. Such satellites are abundant in electron-excited XES [10], and the first such excitations are allowed at our highest excitation energy (751.4 eV). This satellite disappears as the excitation energy is lowered below the threshold for multiple excitations.

While the electronic final states in PES and XES are the same, relative shifts and different broadening of PES and XES features can be attributed to different vibrational dynamics. We observe that the XES features are broader than the corresponding PES features. As the S–F bond has ionic character, it is expected to weaken by the removal of a F 1s electron, an expectation that is supported by DFT, as seen in the molecular dynamics simulations presented below. Coupling to anti-symmetric vibrational modes may lower the electronic symmetry and localize the core hole to one of the fluorine atoms. In case of substantial nuclear rearrangement the scattering process may be regarded as incoherent in the sense that the original inversion symmetry becomes irrelevant for the interpretation. If the XES signal emanates from a fluorine atom with a prolonged S–F bond in a distorted molecule which has lost the  $O_h$  symmetry, the final states would represent holes in valence orbitals that to some degree are localized at this specific fluorine atom, rather than electronically inversion-symmetric orbitals. Picturing molecular orbitals as a linear combination of atomic orbitals a prolongation of the S–F distance implies decreasing overlap between atomic orbitals and consequently a decreasing energy spacing. However, although our molecular dynamics simulation (see inset in figure 3) confirms that the bond associated with the ionized atom is prolonged (reaching 2 Å after only 10 fs) upon core ionization, the reduced spacing in XES as compared to PES is related to changes in intensity due to rehybridization rather than reduced covalent splitting of bonding and anti-bonding orbitals. The symmetry assignment of the calculated XES ( $t = 0$ ) is presented at the bottom of figure 3. In terms of local symmetry, the  $5a_{1g}$ , and  $3e_g$  are of pure  $\sigma$  symmetry, whereas  $4t_{1u}$  and  $5t_{1u}$  are dominated by  $\sigma$  and  $\pi$ , respectively. The other features  $1t_{2g}$ ,  $1t_{2u}$  and  $1t_{1g}$  have  $\pi$  symmetry. The change in spectral shape is followed along the core-ionized state dynamics. For the geometry at 10 fs, many features have shifted and lost most of their intensity due to the elongation (breaking) of the S–F bond to the core-ionized F atom and only one low energy  $\sigma$  and two degenerate high-energy  $\pi$  features remain. At full dissociation into  $\text{SF}_5$  and F fragments and neglecting spin–orbit coupling, these will merge into a single feature due to the spherical symmetry to the F atom. At long time evolution 6–10 fs, we observe a narrowing of the spacing between

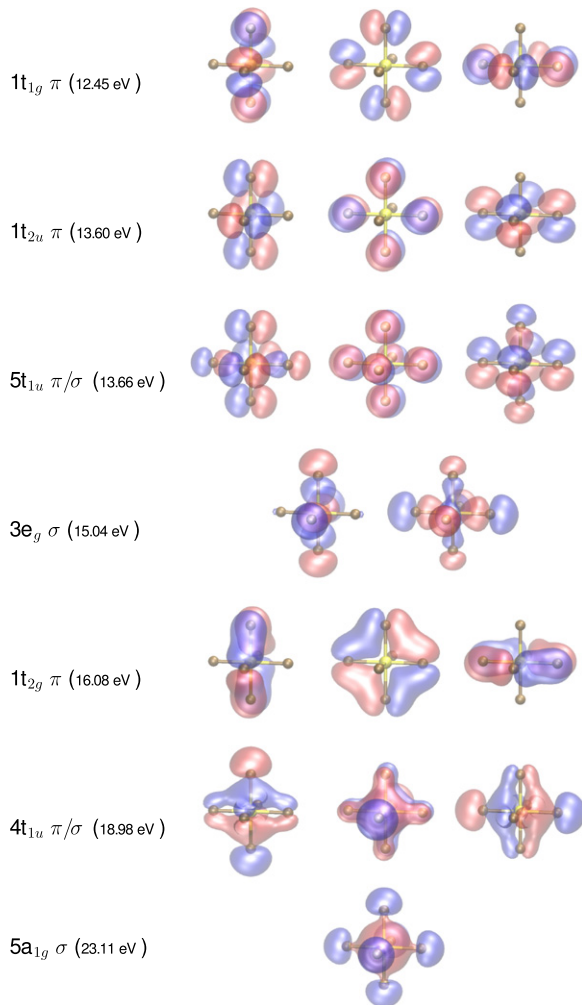


**Figure 2.** Occupied Kohn–Sham molecular orbitals with F 2p and S character classified according to  $O_h$  symmetry and according to their local symmetry around the S–F bonds. Note that the orbital scheme challenges the simplifying ionic-bond picture, and that the  $3e_g$  and  $1t_{2g}$  orbitals have significant sulfur d character.

the  $\sigma$  and  $\pi$  features as a consequence of the reduced overlap between S and F. In figure 3 we see that overall the spectral features both change in intensity and red-shift in emission energy as a function of distortion. In this classical analysis of dynamical effects in XES [25], it is assumed that the measured spectrum comprises features due to transitions at various times during the life of the core hole. As a consequence, the features associated with the  $\sigma$  bonding orbitals in the low-energy part of the spectrum are due to early transitions at relatively short S–F distance, whereas the main feature has a large contribution from later transitions at relatively long S–F distance.

In figure 4, the x-ray absorption spectrum is presented in panel figure 4(a) together with the RIXS at different resonances in panels figures 4(b)–(f). To begin with we start by giving attention to the excitation-energy dependence when the energy is tuned to the shape resonances above the ionization limit, corresponding to unoccupied orbitals of  $t_{1u}$ ,  $t_{2g}$ , and  $e_g$  symmetry at 694.6 eV, 699.8 eV, and 713.1 eV, respectively (figures 4(c), (e), (f)). Apart from the expected elimination

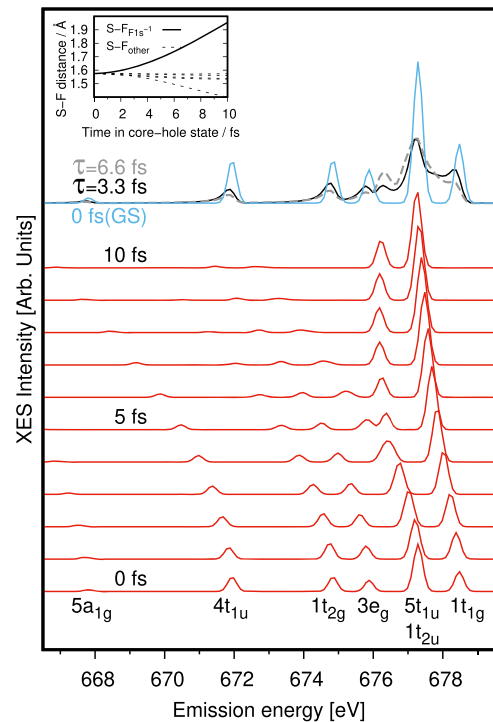


**Figure 3.** Predicted time evolution of the radiative decay (red lines) due to the nuclear dynamics in  $SF_6$  in response to the core-ionization. At the top the life-time averaged XES spectrum (black line) is compared to the neglect of nuclear dynamics (blue line). The evolution in the S–F bond distances is displayed in an inset.

of the high-energy satellite the spectra are very similar to the high-energy excited spectrum, indicating that the excited electron couples only little to rest of the electron system. This is observed in spite of the fact that the final states assigned to the features at 672 eV and 675 eV have different parity,  $4t_{1u}$  and  $1t_{2g}$ , respectively. If inversion symmetry is preserved one expects a relative enhancement of the gerade final state upon resonant excitation of a shape resonance associated with at gerade orbital, i.e., excitation of  $e_g$  (713.1 eV), and  $t_{2g}$  (699.8 eV) would open primarily ungerade core holes, and emission to the gerade  $1t_{2g}$  final state would be enhanced, relative to the ungerade  $4t_{1u}$  state. Conversely, excitation at  $t_{1u}$  (694.6 eV and 696.3 eV) enhances emission to  $4t_{1u}$  relative to the gerade  $1t_{2g}$  final state. We see that this indeed happens in figure 4(d). This implies that the original inversion symmetry does influence the electronic transitions in spite of the coupling to symmetry-breaking vibrational modes. Note, however, that this is a small effect, and one can conclude that the gerade/ungerade selection rule applies only in propensity form.

There is a significant polarization dependence of the relative spectral intensities (figures 4(b), (c), (e), (f)), which can be qualitatively described in both the local and the global symmetric pictures. In the symmetric picture, e.g. excitation of an electron to a gerade  $a_{1g}$  valence orbital can only open a  $t_{1u}$  core hole. With horizontal polarization this implies a combination of core holes primarily on the left and right fluorine atoms, whereas vertical polarization implies a combination of core holes on the up and down atoms. The same site selectivity is



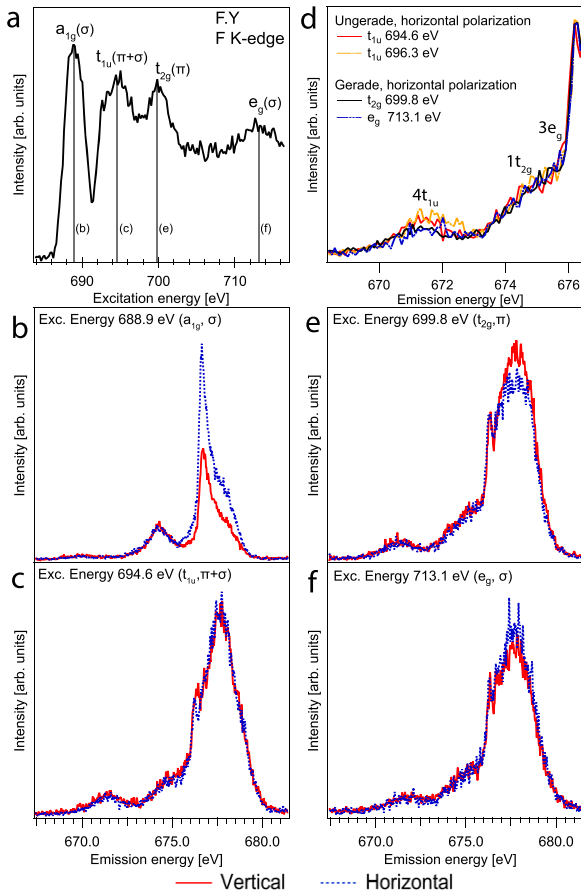


**Figure 4.** Panel (a): the fluorescence yield spectrum, using assignments from reference [22]. Note that the spectrum deviates from an absorption spectrum due to saturation effects, and is used only for reference. Panel (b), (c), (e), (f): RIXS spectra excited with vertical (red) and horizontal (blue) polarization of the incident radiation, at the excitation energies marked with vertical lines in panel (a). A small but significant polarization dependence is observed in panel (e) and (f), while a dramatic effect is observed in panel (b). Panel (d) highlights the excitation-energy dependence of the two well-resolved features that correspond to orbitals of different parity.

expected in a localized picture, considering that the  $a_{1g}$  orbital has local  $\sigma$  symmetry (see figure 2). Here, excitation of a F 1s electron to  $\sigma$  orbital opens a nodal plane perpendicular to the polarization direction, implying that primarily  $\sigma$  orbitals along the bonds in the same direction as the polarization are excited. Horizontal polarization thus primarily excites core holes on the left and right fluorine atoms, whereas vertical polarization excites up and down atoms.

Corresponding considerations apply for the emission. While  $\sigma$  type orbitals radiate primarily perpendicularly to the bond, transitions between orbitals of local  $\pi$  and 1s orbitals radiate also in the bond direction.

Therefore, we expect that in our experimental geometry, horizontal polarization and excitation to resonances of local  $\sigma$  symmetry relatively enhances emission from orbitals of local  $\pi$  symmetry. Analogously, vertical polarization and excitation to resonances of local  $\sigma$  symmetry relatively enhances emission from orbitals of local  $\sigma$  symmetry. The situation is illustrated in figure 5. Similar simplified consideration can be made for

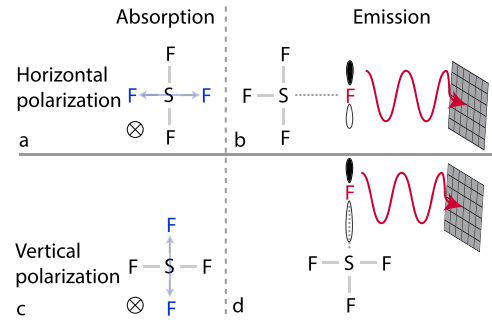


**Figure 5.** A sketch of the  $\pi/\sigma$  asymmetry during breakup. As the first resonance has local  $\sigma$  character horizontal polarization excites the blue atoms left and right (a), so that emission from  $\pi$  orbitals are emphasized in the emission (b). Vertical polarization excites the blue atoms up and down (c) so that also  $\sigma$  orbitals are also observed in the emission (d).

excitation to orbitals of local  $\pi$  symmetry. This primarily selects top and bottom fluorine atoms as well as the front and back atoms. The angular anisotropy is less in this case as both  $\pi$  and  $\sigma$  orbitals radiate perpendicularly to the bond. A rigorous treatment of polarization dependence in RIXS can be found in reference [5].

The observed trends in the polarization dependence (figures 4(b), (c), (e), (f)) are fully in line with this expectation. We recall that the main peak at 678 eV is attributed to final states of predominantly  $\pi$  symmetry, whereas the features below 675 eV are associated with  $\sigma$  bonding states. At 713.1 eV (figure 4(f)) the  $\sigma$  shape resonance is excited, and  $\pi$  emission is relatively enhanced at horizontal polarization. At 699.8 eV (figure 4(e)) the  $\pi$  shape resonance is excited, and  $\pi$  emission is relatively enhanced at vertical polarization. At 694.6 eV (figure 4(c)) the  $t_{1u}$  resonance comprises both  $\pi$  and  $\sigma$  symmetry, and there is no clear polarization dependence at the present level of accuracy.

We can conclude that, while the global inversion symmetry is broken during the scattering process, and gives a slight influence on the spectra, the polarization dependence can be understood in terms of local  $\pi/\sigma$  symmetry.

At 688.9 eV (figure 4(b)) the first unoccupied  $a_{1g}$  orbital is excited. This spectrum takes a form which is dramatically different from spectra excited at higher excitation energies. Both the main peak, corresponding to the nominally non-bonding orbitals of local  $\pi$  symmetry, and the feature corresponding to the  $\sigma$  bonding  $t_{1u}$  orbital becomes sharper, and especially a narrow peak is formed just above 676 eV emission energy. From the electronic decay channel it is well known that ultrafast dissociation occurs upon resonant excitation at the first resonance [14–17], and it is tempting to assign this peak as emission from a free fluorine atom. We note, however, that there is a strong polarization dependence. As a free fluorine atom is spherically symmetric, with a vacancy in the symmetric 1s orbital and a full  $n = 2$  shell, we expect no angular anisotropy in the radiative decay. According to the discussion above, the polarization dependence of relative intensities is due to the selection of atomic centres; left/right for horizontal polarization and up/down for vertical polarization. Together with the symmetry

of the free atom, this picture does not let us expect any polarization dependence. We therefore conclude that the core hole decays during the dynamic dissociation process, and primarily prior to complete separation of the fluorine atom from the molecule.

Then the polarization can be readily understood if the  $\pi/\sigma$  symmetry is considered to be retained. Horizontal polarization preferentially excites the left and right atoms (blue atoms in figure 5(a)). In the geometry of our experimental set-up the radiation of the primarily non-bonding  $\pi$  orbitals is enhanced in the bond direction, which coincides with the direction of the spectrometer. These orbitals simulate 2p orbitals of a free fluorine atom (red atom in figure 5(b)) also before complete dissociation, and one may expect a corresponding sharp atomic-like peak in the emission spectrum. This simple consideration is consistent with the notion that the potential surfaces of a local core hole state and a state with a hole in a local non-bonding ( $\pi$ ) orbital are similar, implying a sharp emission peak and only little vibrational broadening associated with the transition between the two.

At vertical polarization primarily up and down atoms are excited (blue atoms in figure 5(c)). Then emission from bonding  $\sigma$  orbitals are relatively enhanced in our geometry, and their bonding character is retained a larger atomic distances than the non-bonding orbitals (red atom in figure 5(d)). A hole in a bonding ( $\sigma$ ) orbital typically has a potential surface which is significantly different from the core hole state and consequently transitions between the two are accompanied by substantial vibrational excitations. Consequently, the emission spectrum would have a less atomic character than the spectrum excited with horizontal polarization. This simple consideration captures the overall phenomenology. It implies that the sharp line in the spectrum is only quasi-atomic, and that the decay principally occurs before complete dissociation.

The theoretical simulations (figure 3) confirm that there is interaction between the receding atom and the rest of the molecule, also after times longer than the scattering duration, manifested in a  $\sigma/\pi$  splitting. Although this splitting is not observed in the experimental spectra, the interaction is reflected in the polarization anisotropy.

## 5. Conclusion

We have presented and analyzed RIXS spectra of SF<sub>6</sub> excited in the vicinity of the F K edge. Dynamic symmetry breaking is demonstrated in the observation of electronically dipole forbidden states, and the initial-state inversion symmetry influences the spectra only slightly. On the other hand, the local  $\pi/\sigma$  symmetry is crucial for the interpretation of the spectra. Small significant effects are observed for excitation on the sharp shape resonances above the ionization limit, and a dramatic polarization dependence is observed upon excitation to the dissociative first resonance. We attribute this to radiative decay during the dissociation process, where emission from non-bonding orbitals appears atomic while  $\sigma$  orbitals still interact with the molecular fragment.

## Acknowledgments

This work was supported by the Swedish Research Council (VR). The calculations were performed on resources provided by the Swedish National Infrastructure for Computing (SNIC). FG acknowledges support within the Russian Science Foundation (Project No. 16-12-10109).

## ORCID iDs

V Ekholm  <https://orcid.org/0000-0002-3797-3346>

C S  the  <https://orcid.org/0000-0001-7799-8575>

M Simon  <https://orcid.org/0000-0002-2525-5435>

N Jaouen  <https://orcid.org/0000-0003-1781-7669>

M Odelius  <https://orcid.org/0000-0002-7023-2486>

## References

- [1] Domcke W and Cederbaum L 1977 *Chem. Phys.* **25** 189–96
- [2] Malinovskaya S A and Cederbaum L S 2000 *Int. J. Quantum Chem.* **80** 950–7
- [3] Skytt P, Glans P, Guo J H, Gunnelin K, S  the C, Nordgren J, Gel'mukhanov F K, Cesar A and   gren H 1996 *Phys. Rev. Lett.* **77** 5035–8
- [4] Gunnelin K, Glans P, Rubensson J E, S  the C, Nordgren J, Li Y, Gel'mukhanov F and   gren H 1999 *Phys. Rev. Lett.* **83** 1315–8
- [5] Gel'mukhanov F and   gren H 1999 *Phys. Rep.* **312** 87–330
- [6] Lee H W and Kim C S 2001 *Phys. Rev. B* **63** 075306
- [7] Kalozoumis P A, Richoux O, Diakonov F K, Theocharis G and Schmelcher P 2015 *Phys. Rev. B* **92** 014303
- [8] S  derstr  m J et al 2020 *Phys. Rev. A* **101** 062501
- [9] Lavilla R E 1972 *J. Chem. Phys.* **57** 899–909
- [10]   gren H, Nordgren J, Selander L, Nordling C and Siegbahn K 1978 *Phys. Scr.* **18** 499
- [11] Kav  i   M,   itnik M, Bu  ar K, Miheli   A and Bohinc R 2013 *J. Electron Spectrosc. Relat. Phenom.* **188** 47–52
- [12] Kosugi N 2004 *J. Electron Spectrosc. Relat. Phenom.* **137–140** 335–43
- [13] Kivim  ki A, Coreno M, Miotti P, Frassetto F, Poletto L, Str  lman C, de Simone M and Richter R 2016 *J. Electron Spectrosc. Relat. Phenom.* **209** 26–33
- [14] Ueda K et al 1997 *Phys. Rev. Lett.* **79** 3371–4
- [15] Kitajima M et al 2003 *Phys. Rev. Lett.* **91** 213003
- [16] Pr  mper G, Tamenori Y, Fanis A D, Hergenhahn U, Kitajima M, Hoshino M, Tanaka H and Ueda K 2004 *J. Phys. B: At. Mol. Opt. Phys.* **38** 1–10
- [17] Travnikova O, Liu J C, Lindblad A, Nicolas C, S  derstr  m J, Kimberg V, Gel'mukhanov F and Miron C 2010 *Phys. Rev. Lett.* **105** 233001
- [18] Holland D, MacDonald M, Baltzer P, Karlsson L, Lundqvist M, Wannberg B and von Niessen W 1995 *Chem. Phys.* **192** 333–53
- [19] Siegbahn K 1970 *ESCA Applied to Free Molecules* (Amsterdam: North-Holland)
- [20] Chiuzaian S G et al 2014 *Rev. Sci. Instrum.* **85** 043108
- [21] Sacchi M et al 2013 *J. Phys.: Conf. Ser.* **425** 072018
- [22] Hudson E, Shirley D A, Domke M, Remmers G, Puschmann A, Mandel T, Xue C and Kaindl G 1993 *Phys. Rev. A* **47** 361–73
- [23] Shaw R W, Carroll T X and Thomas T D 1973 *J. Am. Chem. Soc.* **95** 5870–5
- [24] Decleva P, Fronzoni G, Kivim  ki A, Ruiz J    and Svensson S 2009 *J. Phys. B: At. Mol. Opt. Phys.* **42** 055102
- [25] Odelius M 2009 *Phys. Rev. B* **79** 144204

- [26] Blum M *et al* 2012 *J. Phys. Chem. B* **116** 13757–64
- [27] The Cp2k Developers Group 2017 Cp2k version 6.0 (development version) <https://cp2k.org>
- [28] Hutter J, Iannuzzi M, Schiffmann F and VandeVondele J 2014 *Wiley Interdiscip. Rev.: Comput. Mol. Sci.* **4** 15–25
- [29] VandeVondele J, Krack M, Mohamed F, Parrinello M, Chassaing T and Hutter J 2005 *Comput. Phys. Commun.* **167** 103–28
- [30] Lippert B G, Hutter J and Parrinello M 1997 *Mol. Phys.* **92** 477–88
- [31] Krack M and Parrinello M 2000 *Phys. Chem. Chem. Phys.* **2** 2105–12
- [32] Adamo C and Barone V 1999 *J. Chem. Phys.* **110** 6158–70
- [33] Guidon M, Hutter J and VandeVondele J 2009 *J. Chem. Theory Comput.* **5** 3010–21
- [34] Kendall R A, Dunning T H Jr and Harrison R J 1992 *J. Chem. Phys.* **96** 6796–806
- [35] Martyna G J and Tuckerman M E 1999 *J. Chem. Phys.* **110** 2810–21
- [36] Herzberg G 1939–1966 *Molecular Spectra and Molecular Structure* (Princeton, NJ: Van Nostrand-Reinhold)
- [37] Iannuzzi M and Hutter J 2007 *Phys. Chem. Chem. Phys.* **9** 1599–610